Optimization of Liquid Scintillator Composition

by

Ayan Batyrkhanov

A Thesis Submitted to the Faculty of the

DEPARTMENT OF PHYSICS

In Partial Fulfillment of the Requirements
For the Degree of

BACHELOR OF SCIENCE

In the School of Science and Technology

NAZARBAYEV UNIVERSITY

2 0 1 7

NAZARBAYEV UNIVERSITY SCHOOL OF SCIENCE AND TECHNOLOGY

As members of the Thesis Committee, we certify that we have read the thesis prepared by Ayan Batyrkhanov entitled

OPTIMIZATION OF LIQUID SCINTILLATOR COMPOSITION

and recommend that it be accepted as fulfilling the thesis requirement for the Degree of Bachelor of Science.

_____ Date: May 8, 2017

Sergiy Bubin

_____ Date: 8/5/17

Dmitriy Beznosko

Final approval and acceptance of this thesis is contingent upon the candidate's submission of the final copies of the thesis to the Department of Physics.

I hereby certify that I have read this thesis prepared under my direction and recommend that it be accepted as fulfilling the thesis requirement.

_____ Date: 11/5/17

Thesis Director: Dmitriy Beznosko

ABSTRACT

Nowadays, many particle detectors use liquid scintillator (LS) as a detection medium. In particular, Water-based Liquid Scintillator (WbLS) that is a new material currently under development. It is based on the idea of dissolving the organic scintillator in water using special surfactants. This material strives to achieve the novel detection techniques by combining the Cherenkov and scintillation light, as well as the total cost reduction compared to pure liquid scintillator.

An important part of either the pure LS or WbLS production is to choose the right fluor and shifter and their concentrations. The choice affects the spectral distribution of the light output and the detection efficiency as each photodetector has its own spectral sensitivity region. This work presents the results of the study on the pseudocumen (PC) based LS with the 2,5-diphenyloxazole (PPO) and 1,4-bis(5-phenyloxazol-2-yl) benzene (POPOP)/1,4-Bis(2-mehylstyryl)benzene (MSB) as a fluor and shifters of choice. Both the total light yield and the spectral differences in the outputs with different amounts of components are shown. This study can be applied to plastic scintillators as well. Typically, each experimental group does the process of scintillator composition optimization per their needs. It is done to minimize the amount of scintillator components used. This research is done in order to assist future experiments in the optimization process.

1. INTRODUCTION

1.1 Scintillation detectors - historic overview

Nowadays particle detectors are used in a wide range of fields such as radiation protection, particle or nuclear physics researches, various medicine applications, etc. Depending on the field of application various types of detectors can be used. Scintillator-based detectors undoubtedly are among the most commonly and widely used charged particle detection devices based on the charged particle producing light in the medium on passage, i.e. scintillation. As described in [1], one of the first examples of scintillator application for charged particle detection was shown in 1903 by Crookes. Instrument consisted of ZnS screen that emitted weak scintillation light when it was hit by alpha-particles. This effect was observed by naked eye. From the same source with the invention of photomultiplier tube (PMT) that was used as the detector of scintillation light, Curran and Baker repeated the Crook's experiment in 1944. At the same time, according to [2], H.P. Kallmann investigated the scintillation properties of large organic crystal made of naphthalene. He demonstrated that it could be used to detect alpha, beta, and gamma radiation. In 1947 Kallmann experimentally discovered that aromatic organic solvents with additional solutes can be used as scintillator as well. His work led to the birth of the modern scintillation detectors.

Scintillators can be made either of organic or inorganic materials [3]. Organic scintillators further subdivide into liquid and solid ones, whereas inorganic scintillators are all solid crystals (e.g. CsI, NaI). Organic and inorganic scintillators differ in light production mechanisms. Liquid and plastic scintillators produce emission light by each single molecule, whereas light from inorganic scintillators depends on the crystal structure. Typically, scintillators behave linearly with respect to the energy deposited, but exhibit quenching at high energy densities. Scintillation light yield is proportional to the excitation energy, at the same time depending linearly on the number of particles in the material. PMT is also a linear device, which makes an electrical signal being proportional to the number of incoming photons up to a certain large threshold (thousands of photons). This linear response property of scintillator makes scintillator detectors easy to use and analyze as compared to others like spark cameras, bubble and cloud chambers. Another useful property of scintillators is fast time response that is short relative to other types of charged particle detectors. It reduces the dead time, i.e. faster recovery of the scintillator material, which, in turn, allows acceptance of higher count rates [1].

Organic scintillator consists of the aromatic hydrocarbon compounds containing benzene ring structures. The most distinguishing feature of these scintillators is very rapid recovery time comparing to other scintillator types.

1.2 Charged particle passage through matter

As a charged particle or high energy photon passes through the medium, transfer of some amount of the energy of the radiation particle or of a photon from the particle to the material takes place. The energy of the passing particle excites atoms or molecules in the medium leading to different energy loss mechanisms, depending on particle species (Figure 1 left). For a charged particle, impart ionization (Figure 1 right) is the most prominent way for energy loss. This radiation makes a so-called 'track', the particle path, while passing through the material. But the effect is very local as majority of the particles in the material will not be affected by ionization [2]. Along the track, production of ions and excited molecules takes place, and depending on their concentration, energy of the primary particle, and interactions, different type of processes can be observed. Some of them are fluorescence, phosphorescence, X-ray emission, energy transfer, etc.

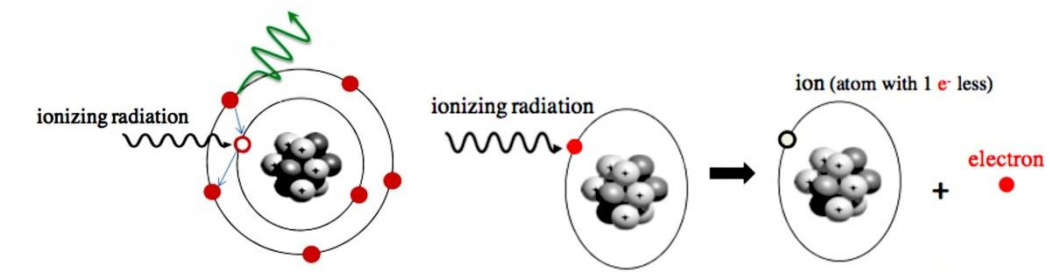

Figure 1. Charged particle interaction with shell electron

Scintillation materials usually undergo photoluminescence process after being excited by ionizing particle. As illustrated in Figure 2, excited electron can make a transition either to singlet excited or to triplet excited state. Electron in singlet excited state is paired with the electron with opposite spin in ground state. Therefore, the transition of the excited electron to the ground state is allowed and accompanied by the photon emission. This process occurs after absorption, within approximately 10^{-8} s, and called fluorescence. However, there is a probability for electron being excited to the triplet excited state. Immediate emission from this state is quantum mechanically forbidden energy state transition and, therefore, the transition to the ground state is delayed. This light emission type is called phosphorescence. [3]

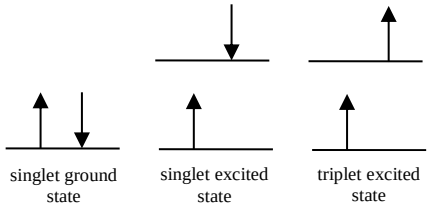

Figure 2. Schematic representation of electron spin configurations in singlet ground, singlet excited, and triplet excited states

Time evolution of re-emission process is described by a two-component exponential, which is linear combination of two exponential decays.

$$N = Aexp\left(-\frac{t}{\tau_f}\right) + Bexp\left(-\frac{t}{\tau_s}\right) \quad (1)$$

where τ_f and τ_s are the fast and slow decay constants, or the prompt and delayed components [1]. Fast component of the decay usually dominates. Amplitudes A and B vary depending on the material, and both of them are related to the mass stopping power, or in other words mean rate of energy loss [4].

Classical formula for energy loss was derived by Niels Bohr in 1922 (Nobel prize). In 1930 and 1932 respectively Hans Bethe corrected the original formula for non-relativistic and relativistic cases. Additional corrections were made by several scientists, but the main contribution was done by Felix Bloch. Therefore, mean energy loss of charged particle passing through the media is described by Bethe-Bloch equation **(2)** [4].

$$\left\langle -\frac{dE}{dx} \right\rangle = Kz^2 \frac{Z}{A}\frac{1}{\beta^2}\left[\frac{1}{2}\ln\frac{2m_e c^2\beta^2\gamma^2 W_{max}}{I^2} - \beta^2 - \frac{\delta(\beta\gamma)}{2}\right], \quad (2)$$

where A is an atomic mass of absorber, i.e. scintillation material, $K = 0.307075\ MeV\ cm^2\ mol^{-1}$, z is an atomic number of incident particle, Z is an atomic number of absorber, I is a characteristic ionization constant (material dependent), $\delta(\beta\gamma)$ is a density effect correction to ionization energy loss, and W_{max} is the maximum energy transfer. In a single collision for particle with mass M it is described by

$$W_{max} = \frac{2m_e c^2 \beta^2 \gamma^2}{1 + 2\gamma m_e/M + (m_e/M)^2} \tag{3}$$

For all practical purposes, $\langle \frac{dE}{dx} \rangle$ for a given material and given particle is only a function of β. Mean energy loss plots for several elements presented in Figure 3, the units of stopping power are $MeV\ g^{-1}cm^2$ [4]. Knowing the material and decay characteristics, pulse shape discrimination can be applied, i.e. incident particle identification.

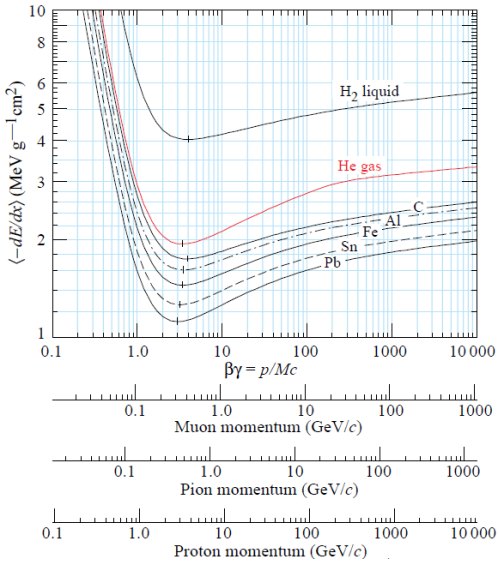

Figure 3. Mean energy loss in liquid H2, He gas, C, Al, Fe, Sn, Pb. Adopted from [4].

1.3 Introduction to liquid scintillator

Organic liquid scintillator is a solution with the aromatic hydrocarbon base. The structure of the solvent is benzene ring. Decay time of such scintillators is very fast, on the order of nanoseconds. Typical solvents for high-energy experiments are toluene, benzene, or 1,2,4-Thimethylbenzene, also known as pseudocumene. Scintillation light in these chemicals is a product of free valence electrons transition. These electrons occupy pi-orbitals, energy diagrams of which is illustrated on Figure 4. Choice of solvent depends on its efficiency characteristic. Light output efficiency of different solvents relative to toluene was discovered by Hayes et al [5].

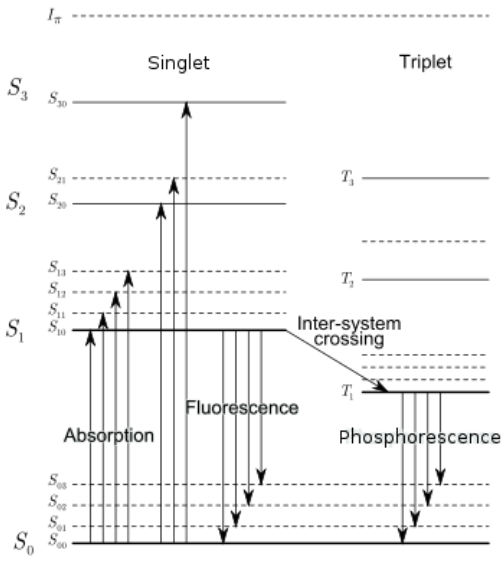

Figure 4. Energy levels for valence electron. Adopted from [6]

Excited pi-electrons undergo fluorescence process and de-excite emitting photons in a longer wavelength. Solvents emit in the UV range (270-320 nm). These photons cannot be detected by most of the photon detectors. Therefore, scintillation light is shifted to more convenient wavelength via solute. Solute, called fluor, is the wavelength shifter, which, in turn, excited by the photon emission from the solvent. Commonly used fluors for scintillator production are PPO (2,5-diphenyloxazole), butyl PBD (2-(4-tert-Butylphenyl)-5-(4-phenylphenyl)-1,3,4-oxadiazole), pterphenyl(1,4-Diphenylbenzene). Absorption spectra of the fluor should coincide with the emission of the base. Re-emission occurs in the visible light range. Wide spread of the absorption and emission photon energies takes place [4], which lead to overlap of these two spectrum (Figure 5). So some fraction of the emitted photons are self-absorbed by the scintillator. This effect causes shortened attenuation length, free path of the light in the material, which leads to lower efficiency. Wavelength distance between the absorption and emission spectrum called Stokes' shift. Increase of this shift is one of the major points of optimization process.

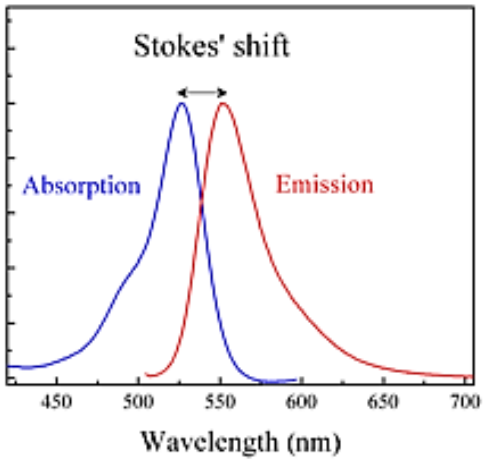

Figure 5. Absorption and emission overlap. Adopted from [7]

In order to avoid spectrum overlapping, another dopant called shifter is added to the scintillator solution. The purpose of additional solute is to shift wavelength of the finally emitted light to the range that does not coincide with the absorption spectra of scintillator. In this case Stokes' shift is increased, and material cannot absorb its own emitted light. Examples of shifter materials are POPOP (1,4-bis(5-phenyloxazol-2-yl)benzene) and MSB (1,4-Bis(2-

mehylstyryl)benzene). Schematic model of the absorption and re-emission process in the scintillation medium consisting of base, fluor and shifter presented in the Figure 6. This re-absorption property of scintillator plays major role in choice of scintillator composition and in the optimization process. Intensity of photons transmitted from the first solute to the second described by the following equation:

$$\boldsymbol{I = fI_0 e^{-lc\epsilon}}, \tag{4}$$

where I_0 is the initial light intensity, f is the overlapping factor, l is the length that photons should pass, c is the scintillator concentration, and ϵ is the extinction coefficient.

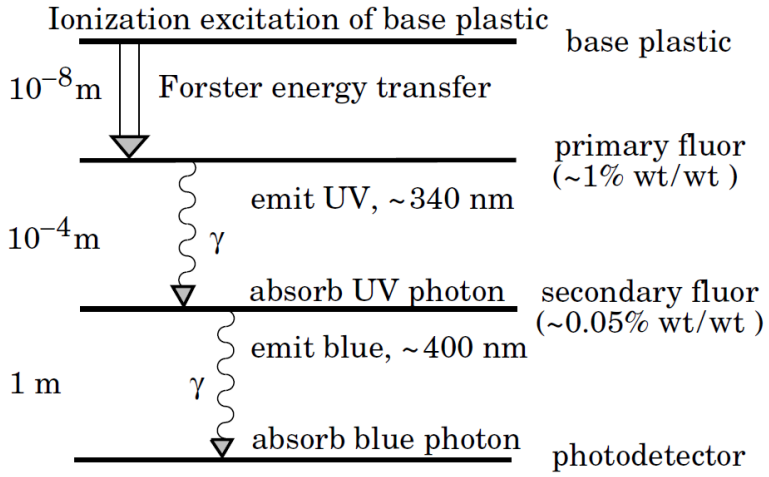

Figure 6. Excitation and emission process in typical scintillator. Adopted from [4]

Although, response of scintillator assumed to be linear with respect to excitation energy, and this approximation considered being good, it is not the case all of the time. Non-linearity occurs because of the recombination and quenching effects that are described well in [2]. Semi-empirical model describing the dependence of light output on the energy losses was suggested by Birks [4].

$$\frac{d\mathcal{L}}{dx} = \mathcal{L}_0 \frac{\frac{dE}{dx}}{1 + k_B \frac{dE}{dx}}, \tag{5}$$

where $\mathcal{L}$ is the luminescence, $\mathcal{L}_0$ is the luminescence at low specific ionization density, $\frac{dE}{dx}$ is the energy losses, and k_B is the Birks' constant that varies for different scintillators.

1.4 Photon detection

Resulting photon emission can be detected by the photomultiplier tube (PMT) [8], either directly or via the wavelength shifting fibers. PMT is the detector of low-level of light intensity in the near-UV and visible parts of spectrum. It converts individual photons into readily measurable electric signals. This class of photon detectors widely used in majority of high-energy physics experiments. Typical scheme of PMT is shown in Figure 7 (left). Other photon detectors types are described in [4]. PMT consists of a photosensitive cathode that is affected by the photons emitted from the scintillator providing photoelectric effect, electron multiplier part (dynodes), and anode [8]. Everything is placed in the glass tube shell. Photoelectrons emitted from the cathode accelerated towards dynodes under applied voltage. Hitting of each consecutive dynode (up to 19 [8]) causes an electron cascade that is finally collected on anode. Current is amplified from 10 to 108 times [8]. Output current signals are in the shape of the pulse that then can be analyzed.

Scintillator and PMT coupling for scintillation counting presented in Figure 7 (right). Overall efficiency of the light yield is the product of efficiency of PMT and internal efficiency of the light emission by each component of the scintillator.

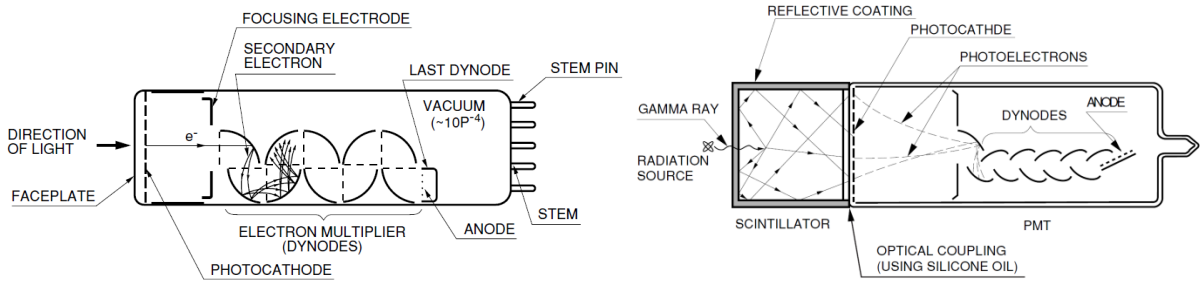

Figure 7. PMT sketch (left) and scintillator and PMT coupling scheme (right). Adopted from [8]

1.5 Liquid scintillator usage in experiments – motivation

Large detection volume and low cost are the main reasons of using LS as a detection medium in many particle detectors. Dissolving LS in water, WbLS can be obtained. It gives an opportunity to detect not only particles, but also the Cherenkov radiation that gives more information on detected particles. Moreover, LS or WbLS composition can be easily changed comparting to plastic ones. Experiments such as Daya Bay use LS. The problem of LS application is optimization process that every experiment does individually for their needs. Motivation of this experiment is to optimize the scintillator composition for future experiments using liquid and plastic scintillators.

The important characteristic in optimization process is the light output of the scintillation. Therefore, light output dependence on the LS concentration was determined. Another factor that effects on the scintillator composition is absorption and emission spectrum of each component. These two major characteristics were investigated in optimization process.

2. FLUOR CONCENTRATION OPTIMIZATION

In order to optimize two-component liquid scintillator it is necessary to start with the fluor first as it is the beginning of light wavelength shifting process.

2.1 LS components

In the experiments, two different compositions of LSs were used: PC+PPO+MSB and PC+PPO+POPOP. The base component for these LSs is 1,2,4-Trimethylbenzene, also known as pseudocumene (PC), with the chemical formula $C_6H_3(CH_3)_3$ and density 876 kg/m^3. PC is in the liquid state and non-soluble in water. 2,5-Diphenyloxazole (PPO) with the chemical formula $C_{15}H_{11}NO$ in the powder form was dissipated in PC. It was used as a primary wavelength shifter and called fluor.

1,4-di-(5-phenyl-2-oxazolyl)-benzene, also known as POPOP, with chemical formula $C_{24}H_{16}N_2O_2$, and 1,4-Bis(2-mehylstyryl)benzene, known as MSB or bis-MSB, with chemical formula $C_{24}H_{22}$ used in the experiments as secondary wavelength shifters. These scintillator components called shifters, and in the powder form are mixed with the base+fluor solution. Both fluor and shifter are non-soluble in water as well.

2.2 Setup description

Scintillation light yield detection setup consists of two MELZ-FEU [9] PMT-115M, CAEN [10] DT5743 Analog-to-digital converter (ADC) and a PMT/sample holder. Holder was designed and printed by myself specifically for this purpose. The structure of the setup is shown in Figure 8. It is designed to house two PMTs facing each other. Test tube with liquid scintillator is placed between PMTs so that the signal can be detected by both.

Figure 8. Schematic of the setup (left) and experiment setup (right)

As was described in the 1.2 scintillation light is the product of charged particle passage through scintillator. Experiment required radioactive particles source for scintillator excitation. Initial tests were done using cosmic rays as a source of radiation. However each data point took several days and also introduced large amount of external noise. Therefore, it was decided to use a ^{60}Co radioactive source tablet to reduce data collection time per sample. For that purpose, holder was designed with the slot for radioactive source tablet under the sample. That resulted in faster data collection that also reduced amount of background noise.

The setup presented in Figure 8 was placed inside the black box for insulation from the background light sources. ADC is used to digitize electric signals from PMTs as well as facilitate the trigger coincidence scheme.

2.3 Optimization procedure

For further uses in experiment, a solution of PPO powder in liquid PC was prepared with a known concentration (29.095 g/L). This solution was further dissolved in 2000 μl of pure PC in order to obtain desired concentrations of PPO. PC+PPO solutions were placed in the setup above. PMTs were connected to voltage source with V=1740 volts. Additional amount of dopant was calculated according to the equation (6). Volumes of tested samples presented in Table 1.

$$\boldsymbol{V_{PPO} = \frac{\omega_f}{\omega_{in} - \omega_f} V_{PC}} \quad (6)$$

where ω_f and ω_{in} are final and initial concentrations of PPO in the sample measured in gram per liter, V_{PC} is the volume of pure PC, V_{PPO} is the volume of PPO added to the PC to obtain desired concentration.

Table 1. Volume of PPO added depending on desired concentration

Concentration, g/L	PPO solution added, μL
0.50±0.005	34.97±0.191
0.75±0.008	52.92±0.303
1.00±0.009	71.19±0.277
1.50±0.043	108.72±3.001
1.75±0.051	127.99±3.601
2.00±0.059	147.63±4.201
2.25±0.067	167.63±4.801
2.50±0.075	188.01±5.401
2.75±0.082	208.77±6.001
3.00±0.090	229.93±6.601
4.00±0.043	318.79±2.482
5.00±0.053	415.02±3.281
6.00±0.063	519.59±4.081

All samples were measured for about 2 minutes each, until ~20,000 data points were collected.

2.4 Fluor data analysis

In order to reduce PMT dark noise and background contribution, double (or two-fold) coincidence trigger schema of two PMTs is used. Coincidence of two PMT pulses provides needed events discrimination, because of non-coincidence of noises [2].

Data obtained was plotted in the form of histograms. The sample data distributions for different concentrations of PPO in the sample (0.5 g/L and 2.5 g/L) are presented in the Figure 9.

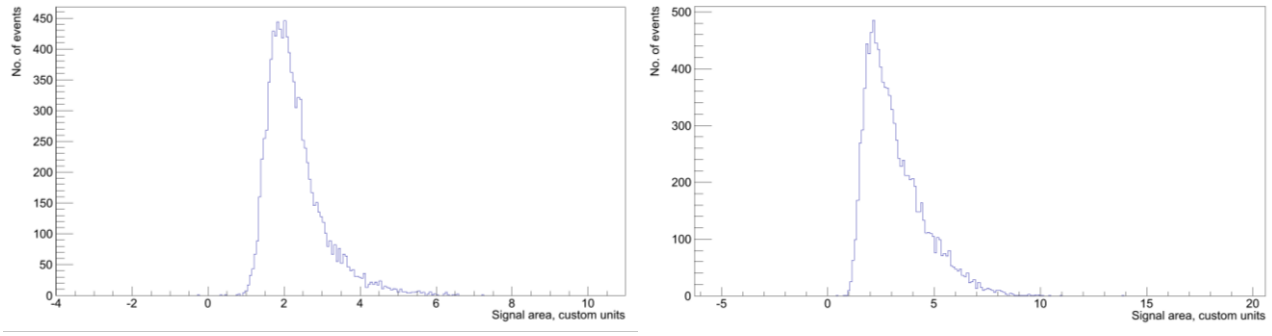

Figure 9. Particle distribution for 0.5 g/L (left) and 2.5 g/L (right) PPO samples

Pure PC sample did not give detectable signal in two-fold coincidence. This result lead us to conclusion that pure PC produces photons with energy above PMT sensitivity region and cannot be detected directly. Addition of PPO to PC shifted light down from UV spectrum range. However, concentrations below 0.5 g/L did not give detectable signals as well. Therefore, PPO of concentration 0.5 g/L was chosen as the starting point for analysis.

Resulting histograms were fitted by Landau distribution that best describes the particle passage through a thin target. Result of statistical analysis is shown in the Figure 10 below. Analysis code can be found in Appendix B.

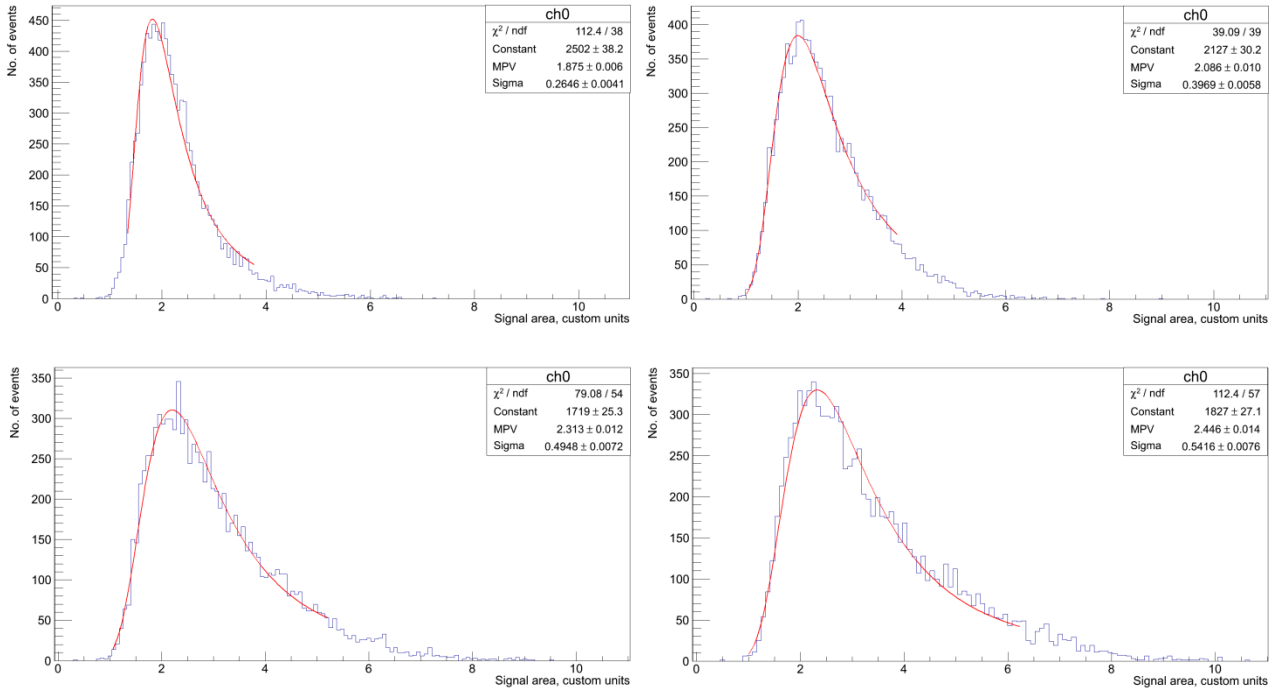

Figure 10. LS light yield analysis of 0.5 g/L (top left), 1 g/L (top right), 2 g/L (bottom left), and 3 g/L (bottom right) PPO samples

MPV variable in the statistics box of Figure 10 represents most probable value that is taken as a measurement of light amount re-emitted by LS. To optimize PPO concentration, the relationship between concentration and MPV was analyzed. Graph of light yield vs. concentration of PPO was plotted. Its fit is represented in Figure 11.

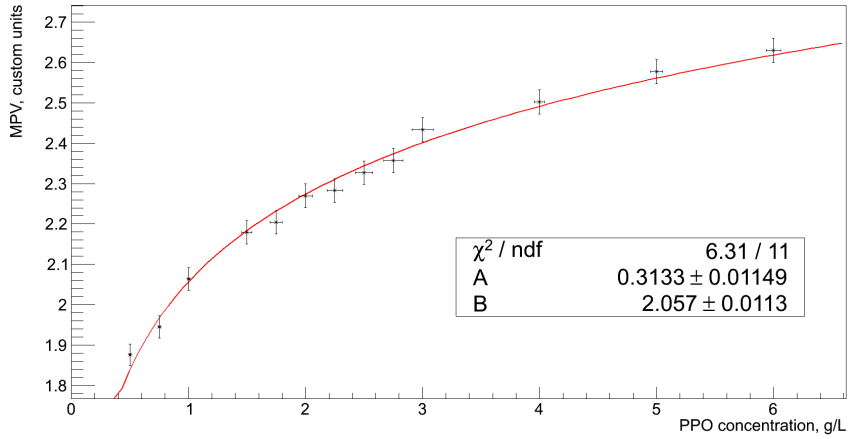

Figure 11. Light yield vs. PPO concentration

As seen from the Figure 11, analysis showed that the relationship between output light and concentration is logarithmic as it was expected initially. Since PPO only shifts some percentage of the pre-existing light emitted by PPO, we expect a saturation to exist when all of available light is being absorbed by the fluor and further addition of it will not change light yield (note that very large concentrations to PPO will actually reduce light yield but this is not studied here). This result establishes that there is no general-case optimal concentration for PC+PPO solution as the slope of logarithmic function decreases monotonously. Sample of PC+PPO with the concentration 2 g/L was chosen for future test as it appears to be widely used. [11]

2.5 Shifter data analysis

Next stage after fluor (PPO) concentration optimization was to optimize the concentration of the shifter. Two options, MSB and POPOP, were chosen as for shifter. Test procedure was same as the PPO optimization process. Amount of additional MSB was calculated using the equation (6). Depending on the desired concentration different volumes presented in Table 2 were added to the PC+PPO solution. As the result of fluor optimization process, PPO concentration of 2 g/L was used.

Table 2. Volume of MSB added depending on desired concentration

Concentration, mg/L	MSB solution added, μL
1.00±0.073	1.99±0.139
2.00±0.052	3.99±0.064
3.00±0.078	5.99±0.096
5.00±0.114	10.00±0.100
7.50±0.166	15.03±0.128
10.00±0.218	20.09±0.152
12.50±0.268	25.17±0.164
15.00±0.320	30.28±0.183
17.50±0.371	35.41±0.194
100.00±4.563	219.37±8.910

According to the calculations, in order to obtain 100 mg/L concentration of MSB in the sample, 219.37 μL of MSB should be added. However, such large volume of MSB in the sample in turns will change concentration of PPO. Therefore there is no sense of creating sample with concentration of MSB 100 mg/L.

Obtained results of experiments on MSB optimization were analyzed using Landau distribution fits as well and are presented in Figure 12.

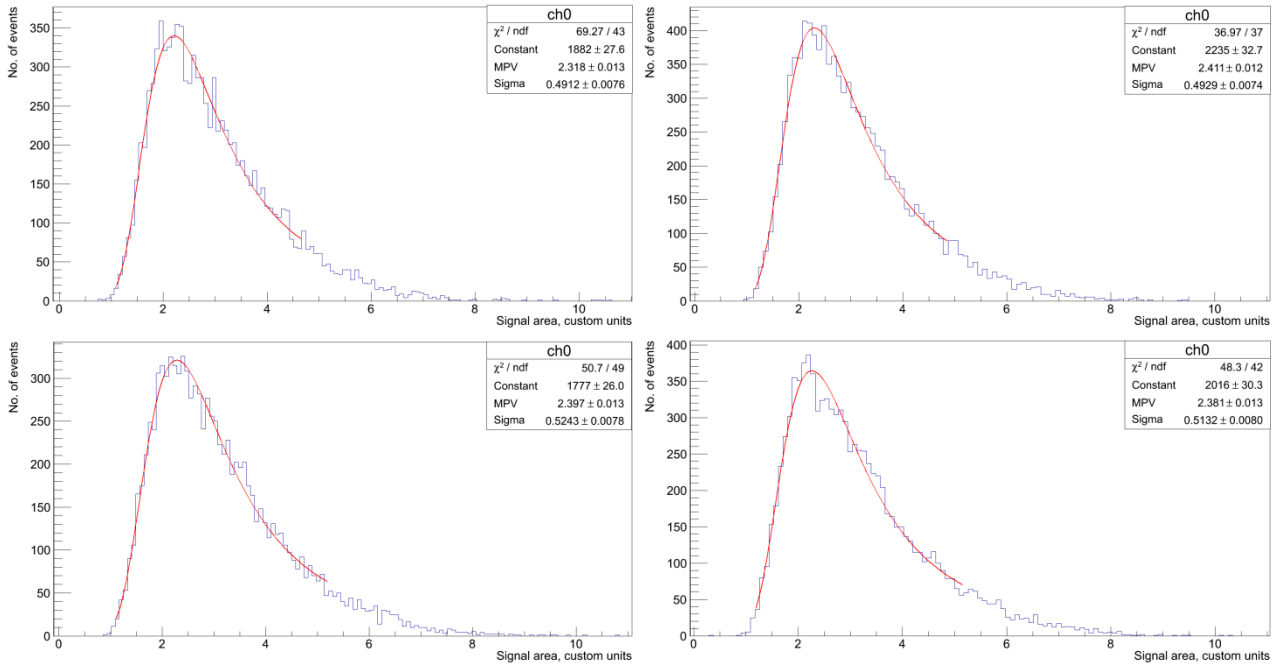

Figure 12. LS light yield analysis of 2 mg/L (top left), 5 mg/L (top right), 10 mg/L (bottom left), and 15 mg/L (bottom right) MSB samples

Analysis of the MPV dependence on concentration of MSB in the sample illustrated the following result that is illustrated in Figure 13. Results of the analysis showed that MSB in the PC+PPO sample did not change the light yield significantly. The light yield from PC+PPO solution was 2.313, while 2 mg/L solution of PC+PPO+MSB resulted 2.318. As it can be seen from the Figure 13, further addition of MSB to the PC+PPO sample caused decrease in the total amount of light detected by PMTs after concentration of 5 mg/L. [11]

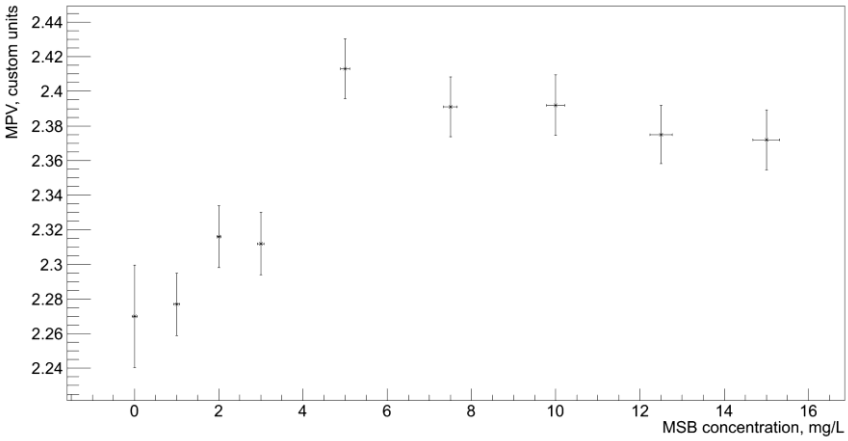

Figure 13. Light yield vs. MSB concentration

This unexpected result was explained by spectral sensitivity of PMTs used in the experiments. Between ~380 and ~410 nm it has almost uniform sensitivity. As far as addition of PPO to PC caused light shifting from UV to ~380 nm, there was no problem with the detection of light emitted by PPO light. However, in the first approximation the MSB is shifting light from PPO to that range of uniform sensitivity (~410 nm). This conclusion has warranted detailed study of the spectral distributions of the LS components. [11]

3. SPECTROSCOPY AND SHIFTER CONTRIBUTION

3.1 Setup description

Measurements of output spectra of LS components were done using Agilent [12] Cary Eclipse spectrophotometer (Figure 14). Setup settings and used parameters of the samples presented in the Table 3 below.

Table 3. Spectroscopy settings

Sample volume, µL	Excitation wavelength, nm	Read-out wavelength range, nm	Excitation slit width, nm	Read-out slit width, nm	Voltage	Read-out speed
800	275	300-550	2.5	5	Medium setting (600V)	Slow setting (~2 min)

Value of sample volume (800 µL) was held constant throughout the whole experiment. Wavelength of the excitation light was chosen at 275 nm to minimally affect the added shifter and excite only fluor molecules.

Figure 14. Spectrophotometer

3.2 Spectrum of the components

Spectra of each component of LS were obtained to further determine its contribution in the LS spectra. These results can be found in Appendix A. Preparation of samples was conducted following the procedure from the sections 2.3 and 2.5.

Experiments showed that in the PC+PPO sample PPO shifts incoming light at ~380 nm, while PC itself has negligible contribution in light yield. This process is illustrated in the Figure 15.

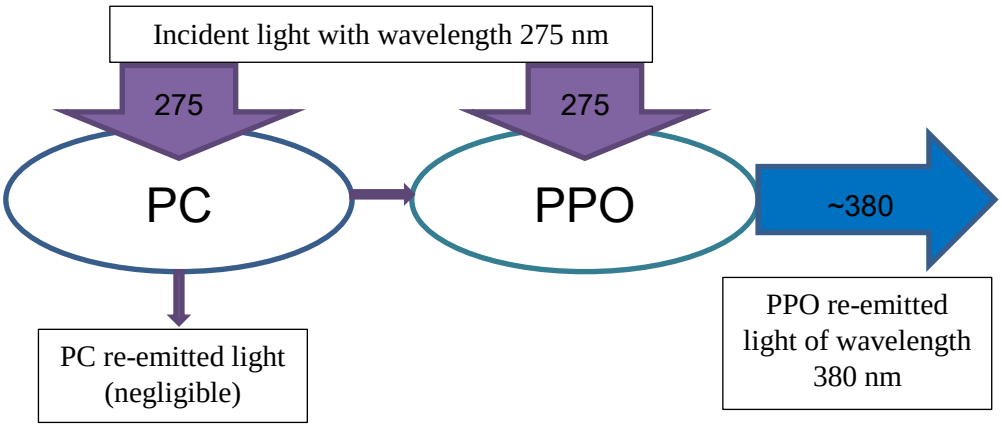

Figure 15. Schematic representation of PC+PPO light re-emission

Addition of MSB or POPOP furthers the shifting process. The spectrum shapes for different concentrations of POPOP in LS are presented in the Appendix A. Experimental results showed that 275 nm light almost did not excite shifter component, thus, its contribution to the light output spectra can also be neglected. Output spectrum mainly is the result of the shifter re-emission, mechanism of which is illustrated in the Figure 16.

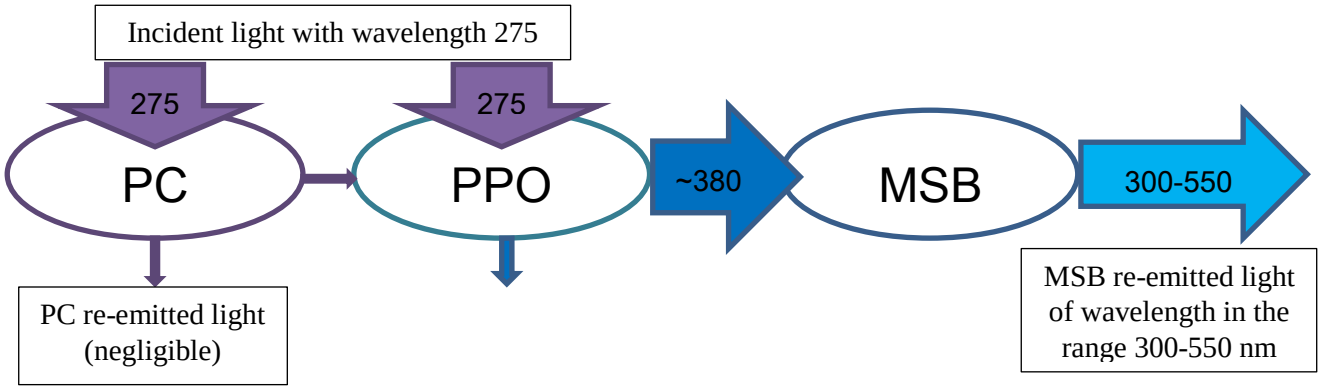

Figure 16. Schematic representation of PC+PPO+MSB light re-emission

3.3 Spectrum analysis

To combine absorption and emission spectrum the following empirical equation was used:

$$(A - B * [MSB_{abs}]) * [PPO_{em}] + C * [MSB_{em}] + D * [PC_{em}], \quad (7)$$

where quantities in the square brackets represents the data points of the respective component; $[MSB_{abs}]$ is the absorption spectra of the MSB excited by PPO emitted light (350 nm); $[PPO_{em}]$ is the emission spectra of PPO, excited at 275 nm; $[MSB_{em}]$ is the re-emission of MSB light emitted by PPO; $[PC_{em}]$ is the emission spectra of pure PC in the sample; A, B, C and D are the parameters that represent the contribution of each component to the output emission spectra.

All spectra of the components were averaged and then used to make fit of the light emitted by the sample (Appendix A: Figure A.13). Some of the resulting plots for MSB concentrations 2 mg/L, 4 mg/L, 6 mg/L, and 8 mg/L are presented in the Figure 17 below.

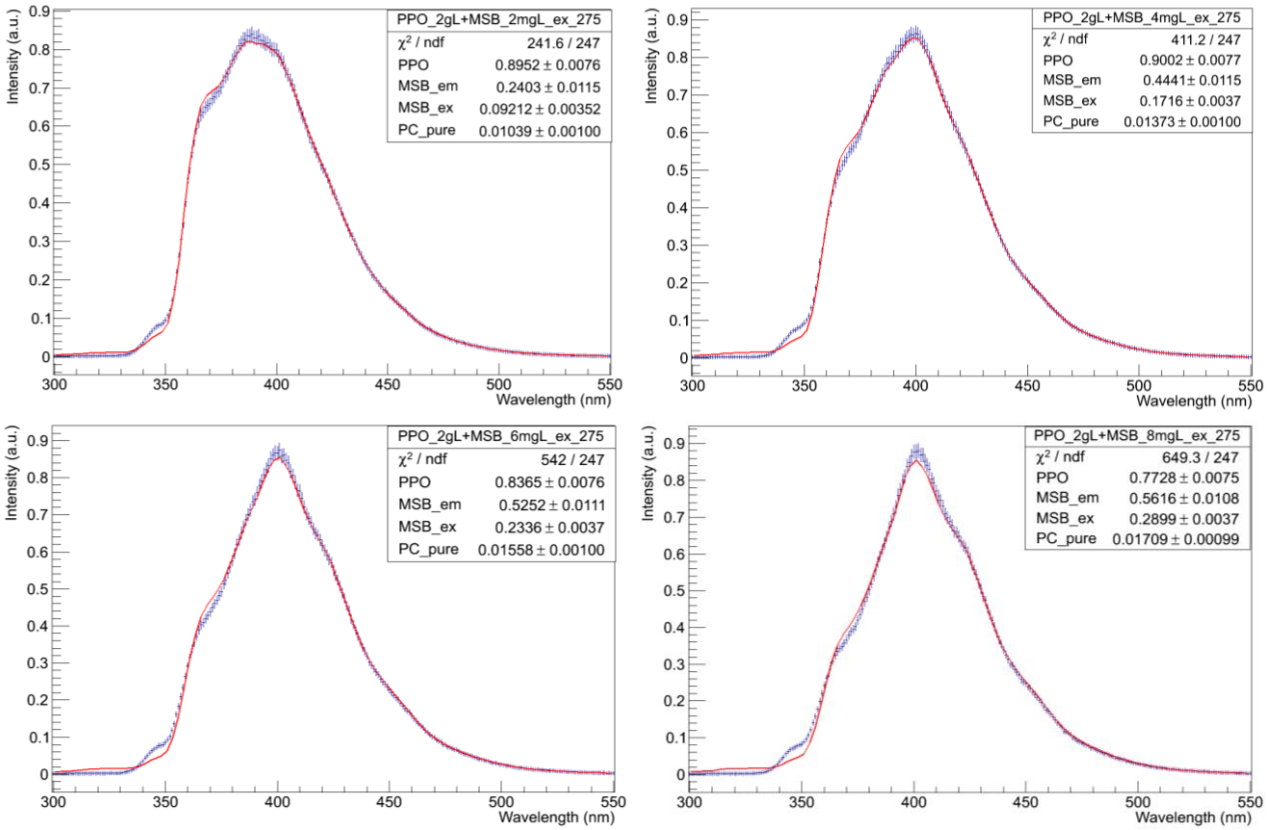

Figure 17. Emission spectra fit of the samples PC+PPO+MSB 2 mg/L (top left), PC+PPO+MSB 4 mg/L (top right), PC+PPO+MSB 6 mg/L (bottom left), and PC+PPO+MSB 8 mg/L (bottom right) excited at 275 nm

Parameters A, B, C and D from the equation (7) represent the *PPO*, *MSB_em*, *MSB_ex*, and *PC_pure* parameters in the statistics box of the Figure 17. *PPO*, *MSB_em*, *MSB_ex*, and *PC_pure* are the parameters for the PPO re-emitted light, MSB absorption spectra, MSB re-emission spectra, and contribution of pure PC and other background noise in the output emission spectra of the sample.

Parameters of the most interest are MSB_em and MSB_ex. Ratio of these two parameters shows that only 40-50% of the light absorbed by MSB from PPO emission is re-emitted. Therefore, integral light yield is reduced. [11]

Conclusion

The work has been done on the optimization of LS composition. The results can be applied to plastic scintillators as well. Concentration of each LS component can be chosen based on the needs from the fit parameters of the light yield. Experiment showed that the amount of output light is reduced when the shifter is added to the base + fluor solution as shifter efficiency is ~45%. This result was confirmed by experiments on spectroscopy as well as on direct detection of light yield by two-fold coincident PMTs. The choice of the shifter depends on the sensitivity of the detector used for the experiment.

This study plans to continue the work creating the data base and software that can be used to optimize the scintillator composition by fitting its expectative output spectrum. This software will be useful for future experiments using plastic or liquid scintillators.

BIBLIOGRAPHY

[1] W. Leo, Techniques for Nuclear and Particle Physics Experiments, Berlin Heidelberg: Springer-Verlag, 1987.

[2] D. Horrocks, Applications of Liquid Scintillation Counting, New York and London: Academic Press, 1974.

[3] Adil Baitenov, Alexander Iakovlev, Dmitriy Beznosko, "Technical manual: a survey of scintillating medium for high-energy particle detection," *arXiv:1601.00086*, 2016/1/1.

[4] C. Patrignami et al. (Particle Data Group), Chinese Physics C, 40, 100001 (2016).

[5] F.N. Hayes, B.S. Rogers, R. Sanders, R.L. Schuch, and D.L. Williams, Rep. LA-1639. Los Alamos Sci. Lab.. Los Alamos, New Mexico, 1953.

[6] "Scintillation(physics)," https://en.wikipedia.org/wiki/Scintillation_(physics).

[7] "Stokes shift," https://en.wikipedia.org/wiki/Stokes_shift.

[8] Hamamatsu Photonics K.K., PHOTOMULTIPLIER TUBES. Basics and Applications, Hamamatsu Photonics K.K. Electron Tube Division, 2007.

[9] MELZ-FEU, Zelenograd, g. Moskva, Russia, 4922-y pr-d, 4c5, 124482 (http://www.meltz-feu.ru).

[10] CAEN, S.p.A. Via della Vetraia, 11, 55049 Viareggio Lucca, Italy (http://www.caen.it).

[11] A. Batyrkhanov, D. Beznosko, A. Iakovlev, K. Yelshibekov, "Optimization of the Liquid Scintillator Composition," in *Proceedings of ICHEP2016 Int., PoS(ICHEP2016)775*, Chicago, 10/2016.

[12] Agilent INC., 5301 Stevens Creek Blvd, Santa Clara, CA 95051, United States (http://agilent.com).

Appendix A

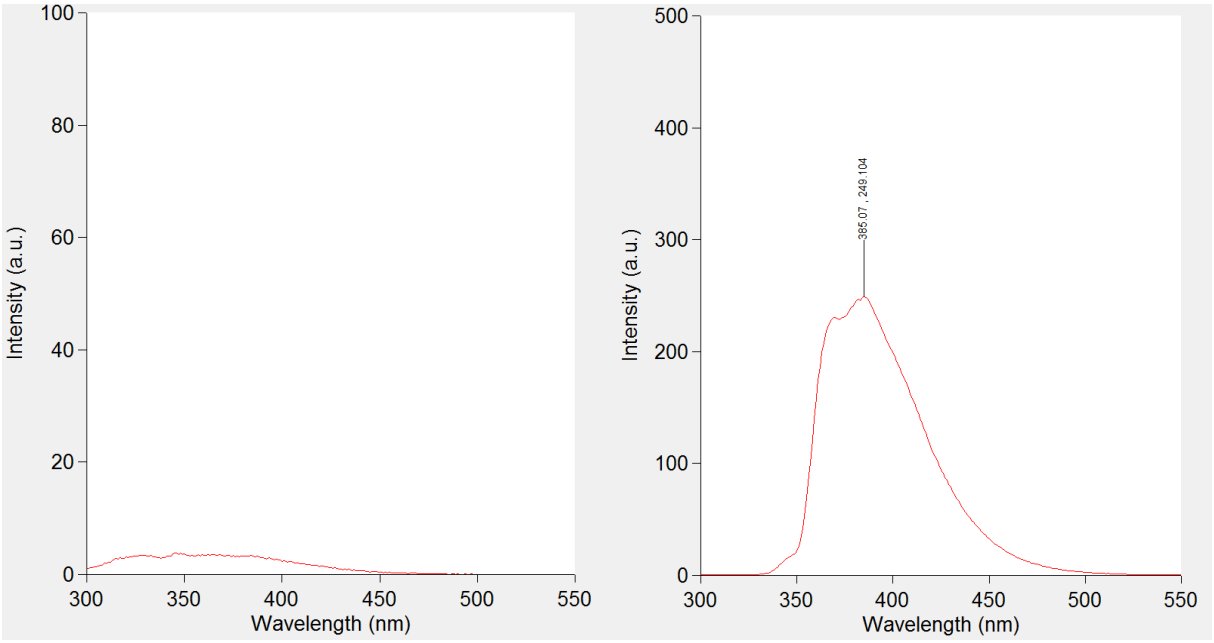

Figure A.1. Pure PC (left) and PC+PPO 2 g/L (right) excited at 275 nm

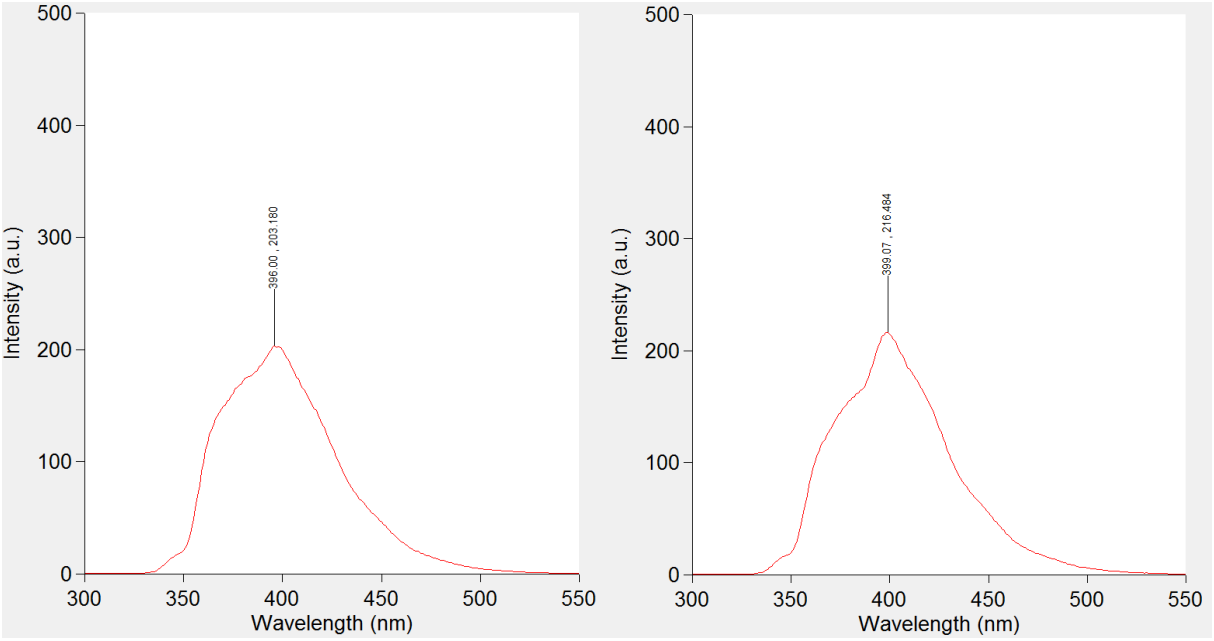

Figure A.2. PC+PPO+POPOP 2 mg/L (left) and PC+PPO+POPOP 3 mg/L (right) excited at 275 nm

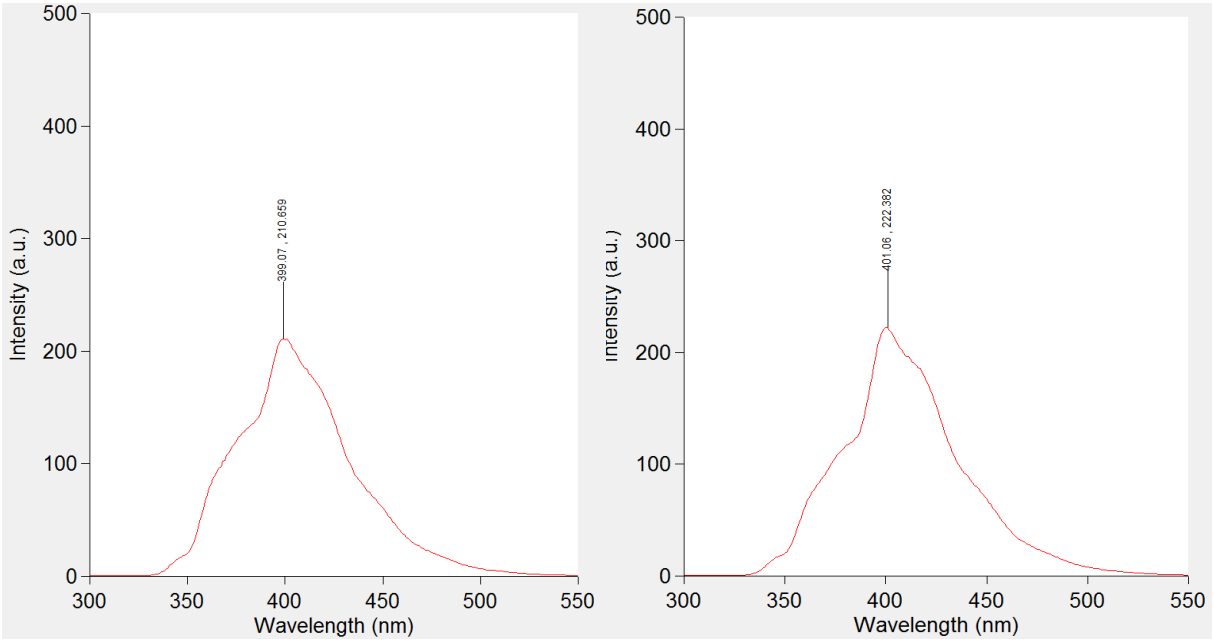

Figure A.3. PC+PPO+POPOP 4 mg/L (left) and PC+PPO+POPOP 5 mg/L (right) excited at 275 nm

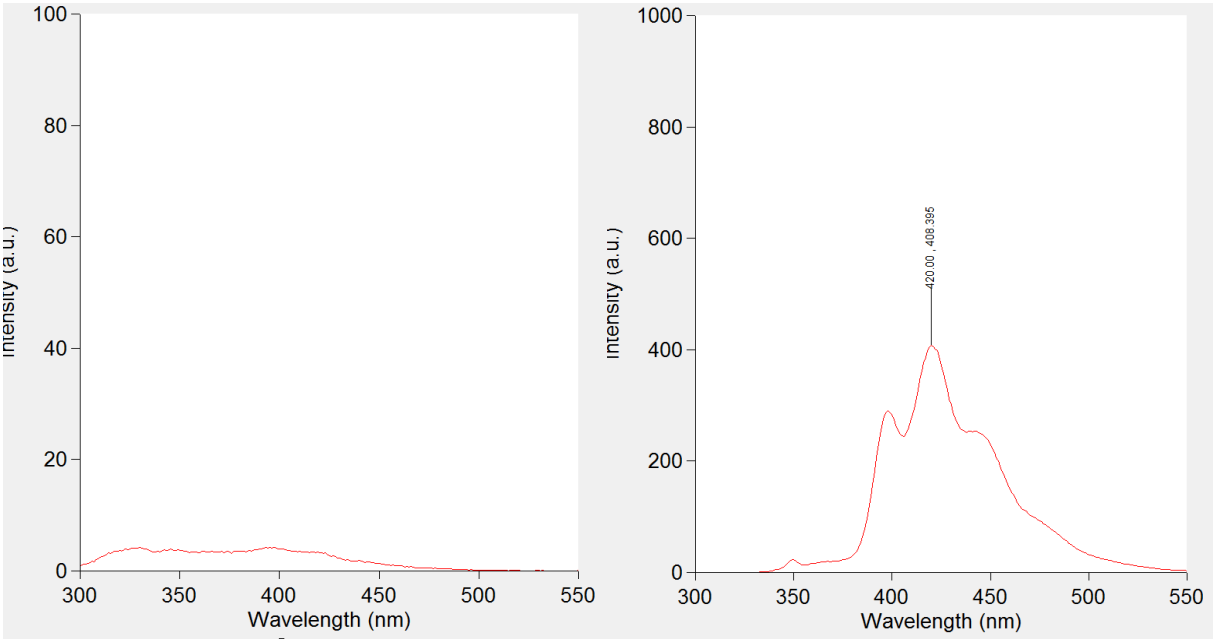

Figure A.4. PC+POPOP 1 mg/L excited at 275 (left) and 350 nm (right)

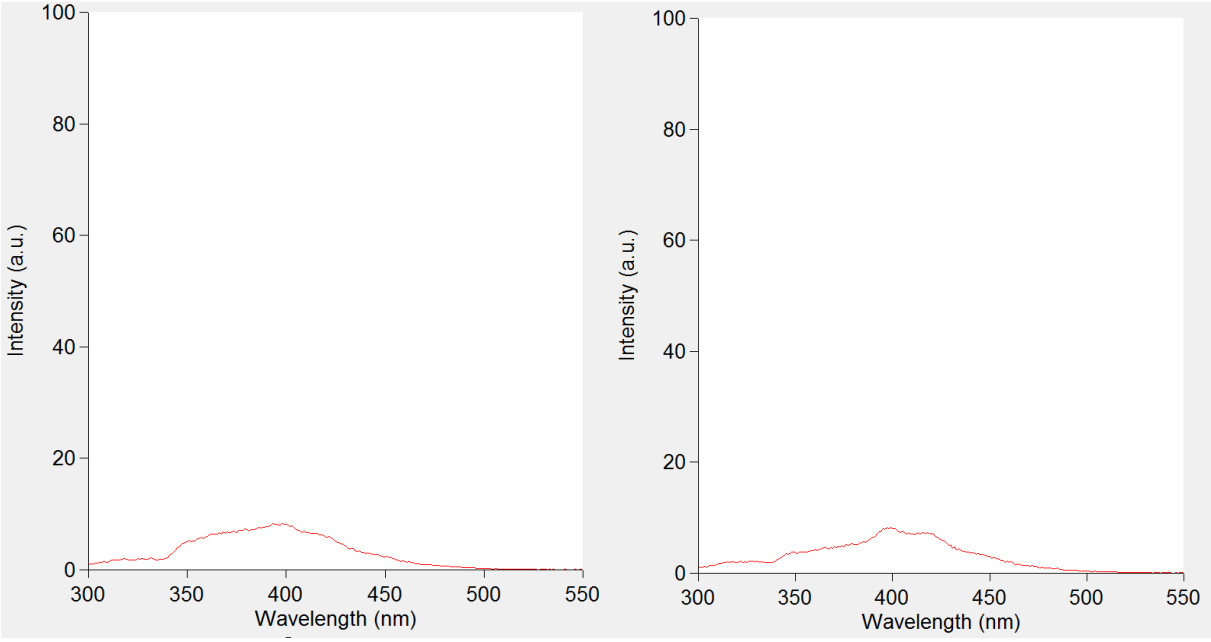

Figure A.5. PC+POPOP 1 mg/L (left) and 2 mg/L (right) excited at 275 nm

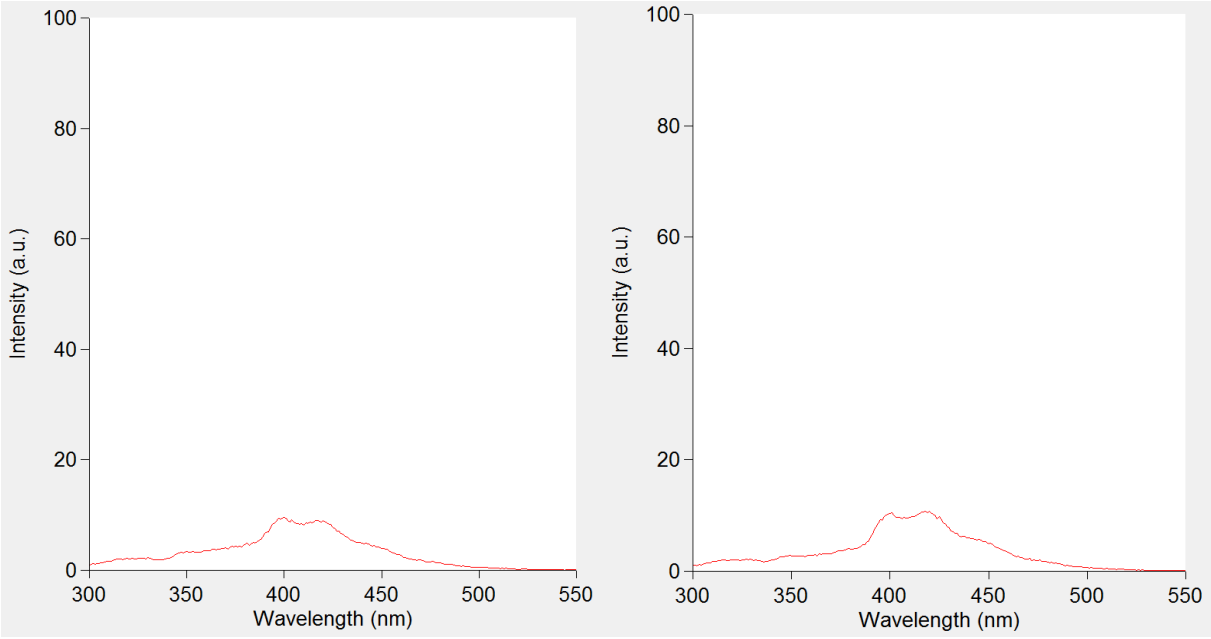

Figure A.6. PC+POPOP 3 mg/L (left) and 4 mg/L (right) excited at 275 nm

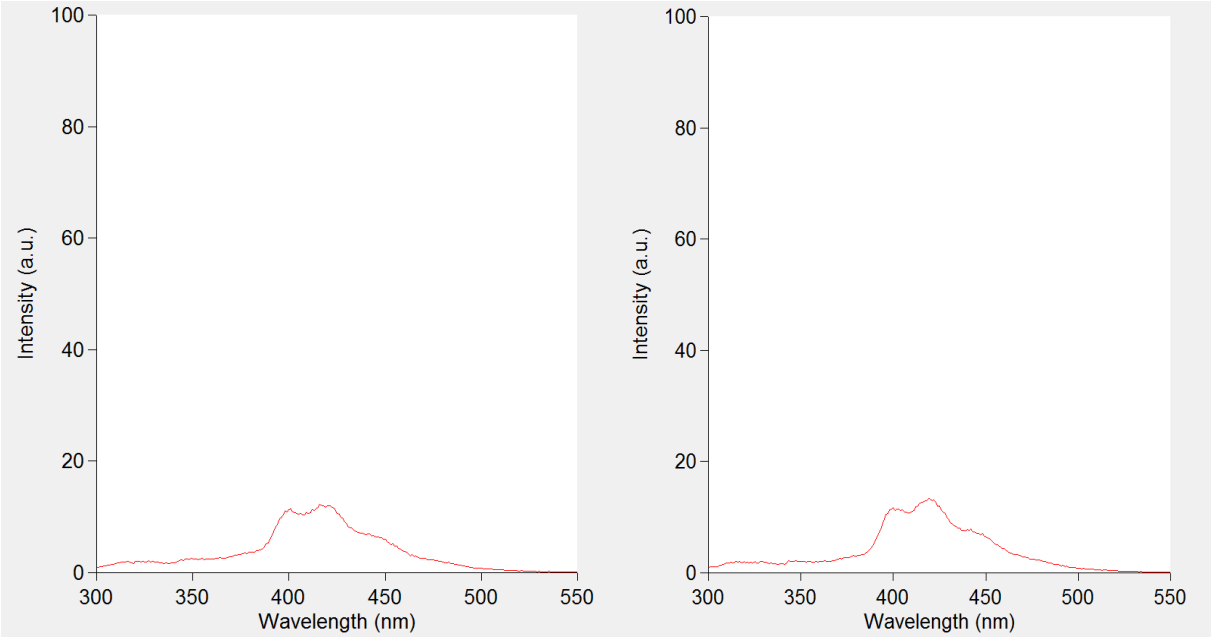

Figure A.7. PC+POPOP 5 mg/L (left) and 6 mg/L (right) excited at 275 nm

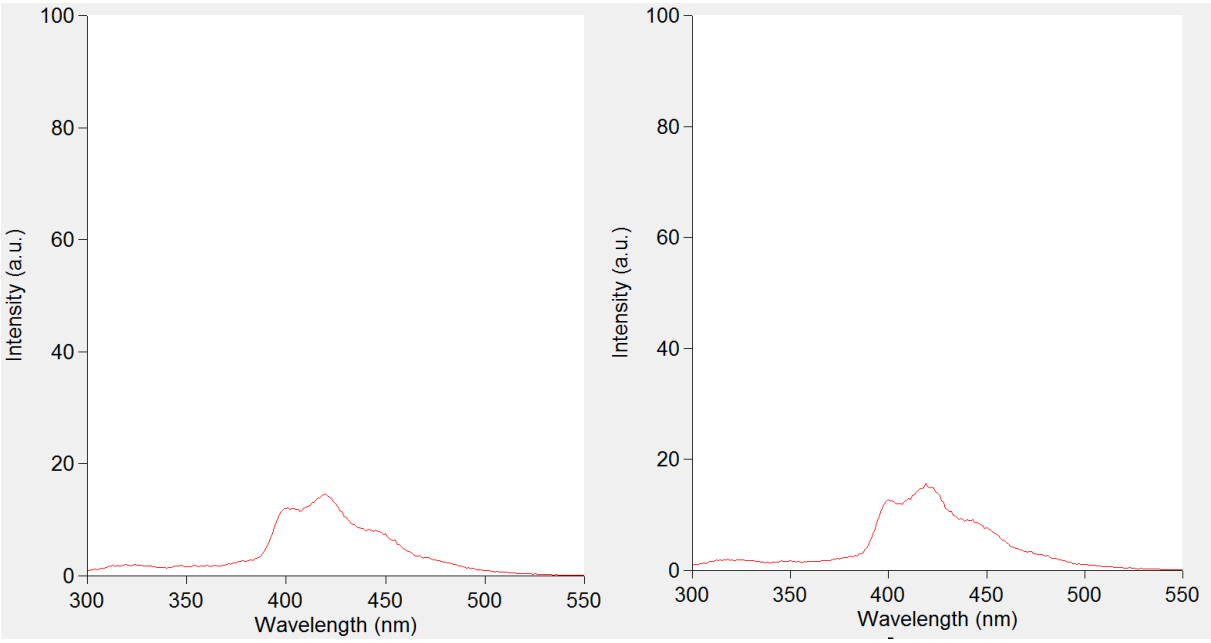

Figure A.8. PC+POPOP 7 mg/L (left) and 8 mg/L (right) excited at 275 nm

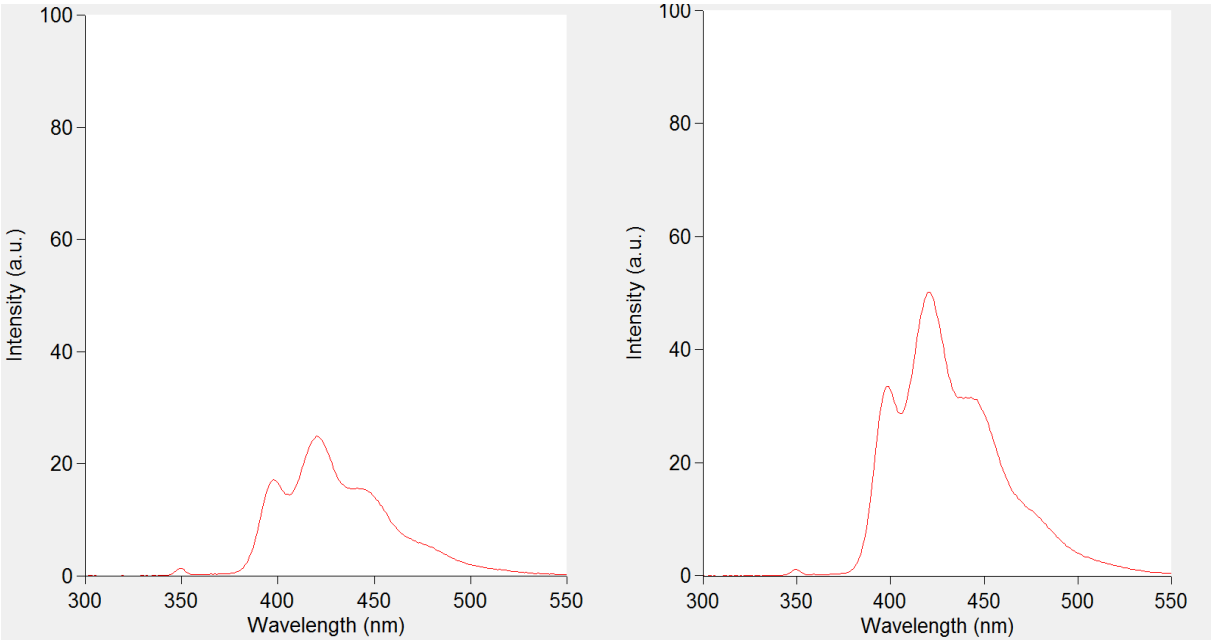

Figure A.9. PC+POPOP 1 mg/L (left) and 2 mg/L (right) excited at 350 nm

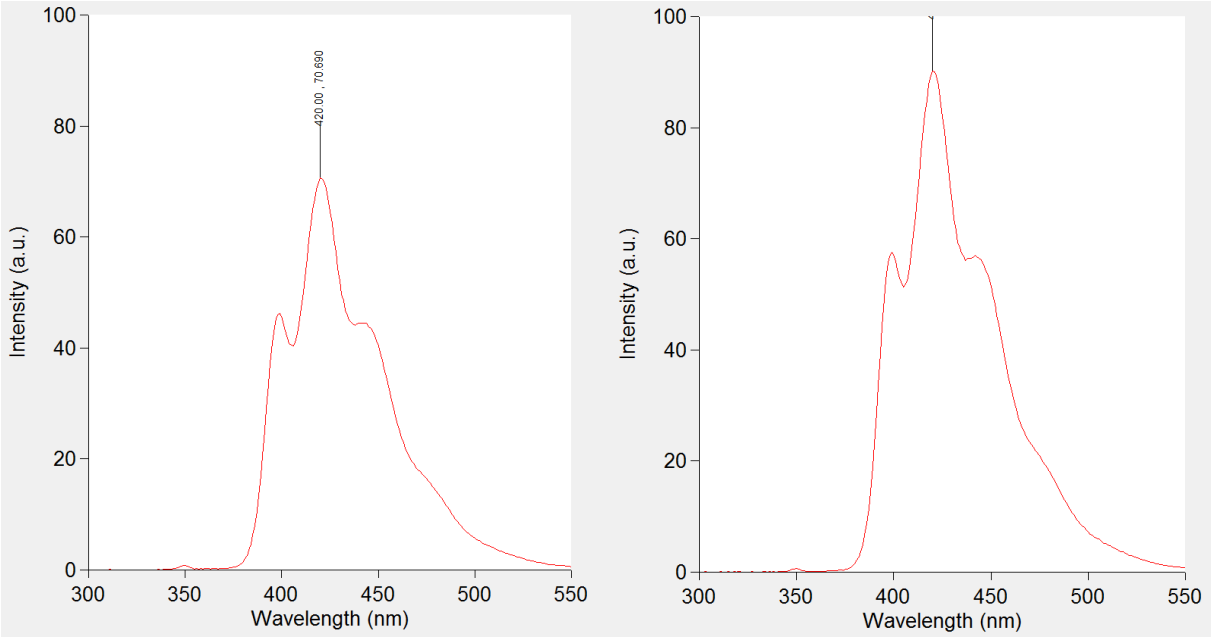

Figure A.10. PC+POPOP 3 mg/L (left) and 4 mg/L (right) excited at 350 nm

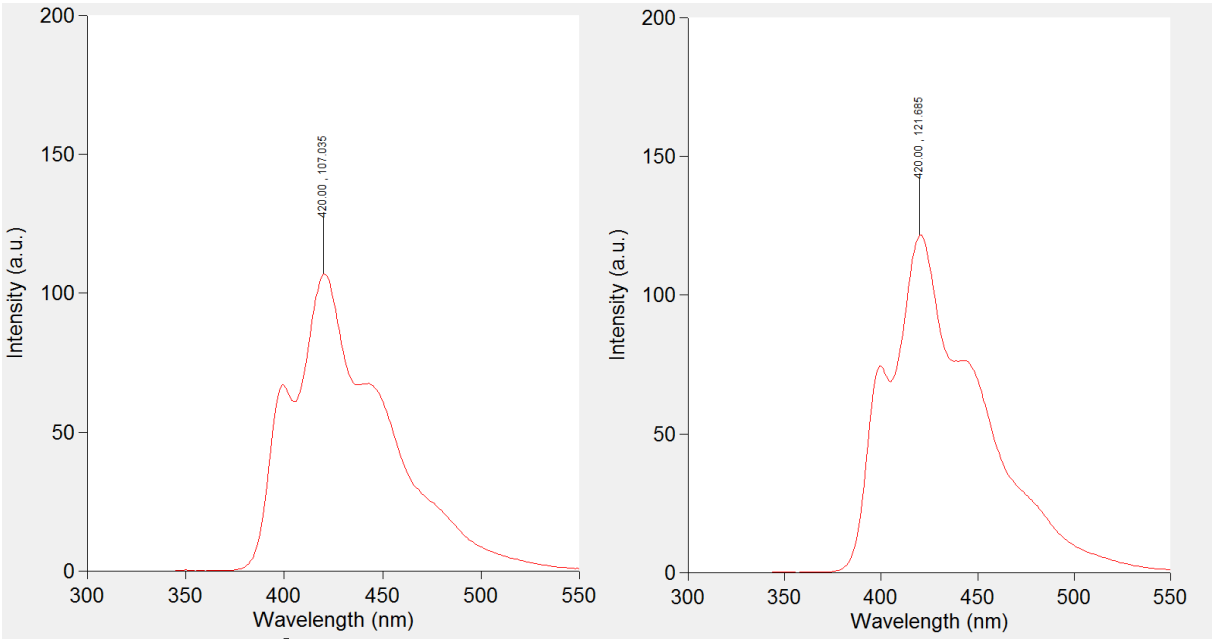

Figure A.11. PC+POPOP 5 mg/L (left) and 6 mg/L (right) excited at 350 nm

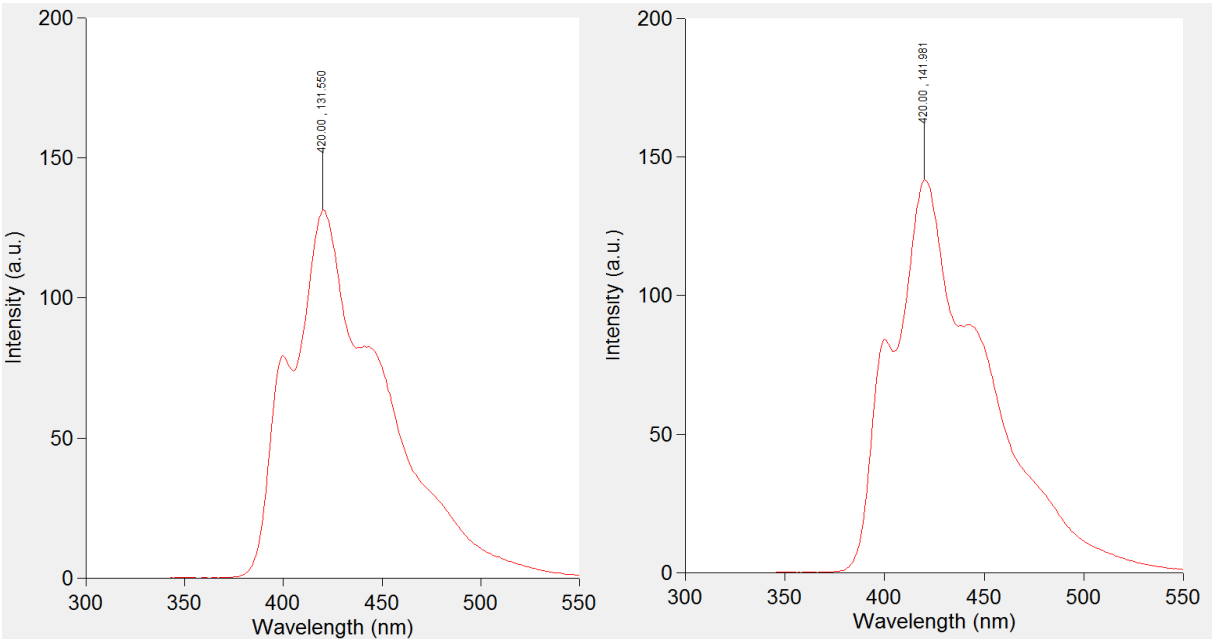

Figure A.12. PC+POPOP 7 mg/L (left) and 8 mg/L (right) excited at 350 nm

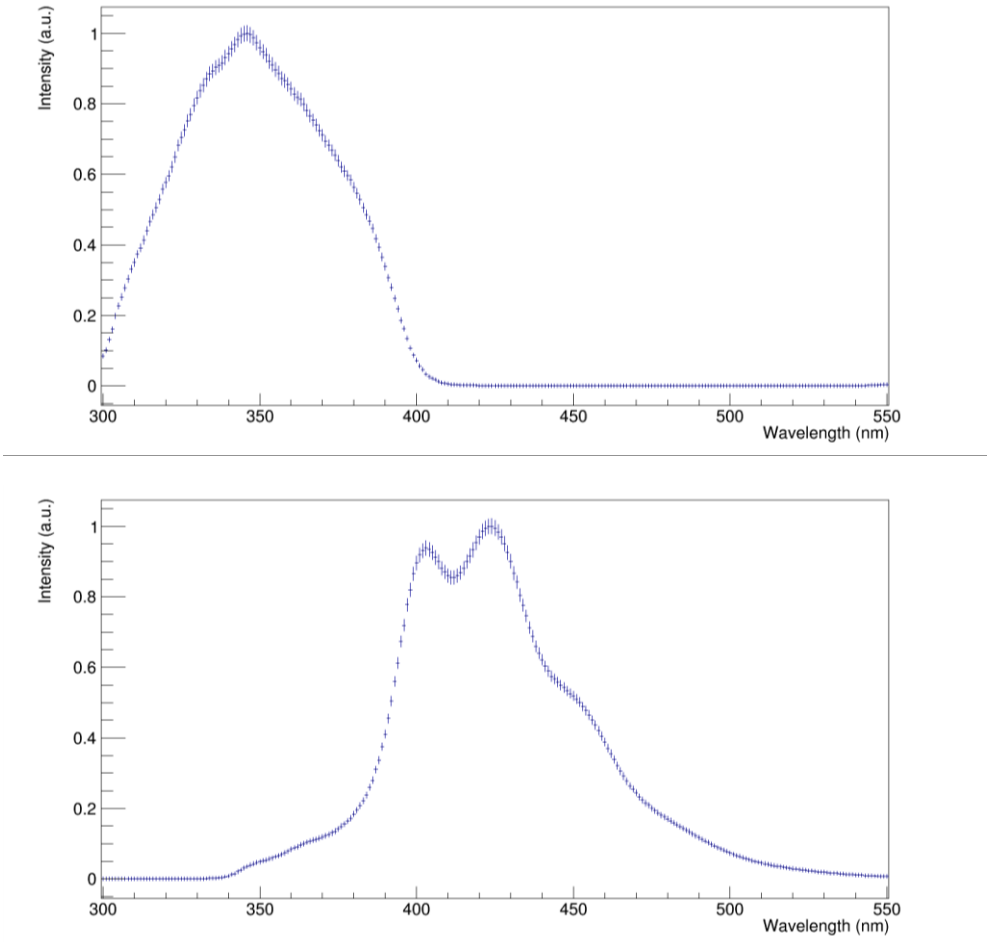

Figure A.13. Weighted average of MSB emission (top) and MSB absorption (bottom) spectrum excited by PPO re-emission

Appendix B

```
from sys import argv, exit
from numpy import array, zeros, sqrt,argmax
import ROOT
if len(argv)<2:
        print 'use as: program.py datafile'
        exit()
file=open(argv[1],'r')
print argv[1],' file opened, starting analysis for 2 histo channels'
tempcounter=0
chdata={}
chdata[5]=[];chdata[7]=[];chdata[13]=[];chdata[15]=[];
for i in file:
        tempcounter+=1
        if tempcounter==5 or tempcounter==13:
                i=i.split(' ')
                for j in i:
                        if not (j==" or j=='\n'):
                                chdata[tempcounter].append(float(j))
        if tempcounter==7 or tempcounter==15:
                i=i.split(' ')
                for j in i:
                        if not (j==" or j=='\n'): chdata[tempcounter].append(int(j))

#now create histos
print len(chdata[5]),-1*max(chdata[5]),-1*min(chdata[5])
ch0h=ROOT.TH1F("ch0","",len(chdata[5]),-1*max(chdata[5]),-1*min(chdata[5]))
ch0h.GetXaxis().SetTitle("Signal area, custom units")
ch0h.GetYaxis().SetTitle("No. of events")

#now set the bins
for i in xrange(0,len(chdata[5])):
        ch0h.SetBinContent(i+1,chdata[7][len(chdata[5])-i-1])

#now plotting
ROOT.gStyle.SetOptFit()
canv=ROOT.TCanvas('data ch','data ch',100,100,1200,500)
maxposition1=argmax(chdata[7])
maxposition2=argmax(chdata[15])
canv.cd; ch0h.Draw();ch0fit=ch0h.Fit("userf1","RS");
canv.Update();canv.Draw();
```

Appendix C

```
import ROOT, numpy, sys

histograms={}
data={}
preset='.csv'
PPO_Area=0
i=0

def Onetracklengthfunc(x,par):
	bin=histograms[PC].GetXaxis().FindBin(x[0])
	func=(par[0]-
par[1]*histograms[MSB_em].GetBinContent(bin))*histograms[PPO].GetBinContent(bin)+par[2]*histogram
s[MSB_ex].GetBinContent(bin)+par[3]*histograms[PC].GetBinContent(bin)
	return func

def Create_histogram(filename):
	global PPO_Area
	data[filename] = numpy.genfromtxt(filename+preset, delimiter=',', skip_header=2, max_rows=251)

	x=[]; y=[]; x_error=[]; y_error=[]
	for i in range(0, len(data[filename])):
		x.append(data[filename][i][0])
		y.append(data[filename][i][1])
	x_error=numpy.zeros(len(x));
	x=numpy.array(x); y=numpy.array(y)

	if filename==PPO:
		PPO_Area=numpy.sum(y)
		max_value=numpy.max(y)
		y=y/max_value

	elif filename==PPO_MSB:
		PPO_MSB_Norm_coff=numpy.max(y)*(PPO_Area/numpy.sum(y))
		y=y/PPO_MSB_Norm_coff

	else:
		max_value=numpy.max(y)
		y=y/max_value

	y_error=y*0.0164+0.005

	histograms[filename] = ROOT.TH1D(filename,filename, len(x), 299.5, 550.5)
	for i in range(0, len(x)):
		histograms[filename].Fill(x[i], y[i])
		bin=histograms[filename].GetXaxis().FindBin(x[i])
		histograms[filename].SetBinError(bin, y_error[i])

def Save_histogram(filename):
	outputfile=ROOT.TFile('Analyzed/'+filename+'.root','recreate')
	if not outputfile.IsOpen():
		print 'problem opening outputfile'
		sys.exit(1)
	histograms[filename].Write()
	outputfile.Close()
	if outputfile.IsOpen():
```

```
                print 'problem closing outputfile'
                sys.exit(1)
        print 'outputfile for '+filename+' created successfully'

def Plot_histogram(filename, i):
        if (filename == PPO_MSB):
                c2.cd(i)
                histograms[filename].SetTitle(filename)
                histograms[filename].GetXaxis().SetTitle("Wavelength (nm)")
                histograms[filename].GetYaxis().SetTitle("Intensity (a.u.)")
                histograms[filename].Fit("fitfunc")
        else:
                c2.cd(i)
                histograms[filename].SetTitle(filename)
                histograms[filename].GetXaxis().SetTitle("Wavelength (nm)")
                histograms[filename].GetYaxis().SetTitle("Intensity (a.u.)")
                histograms[filename].Draw("L")

for density in range(2,9,2):

        PC='PC_pure'
        PPO='PC+PPO_2gL'
        MSB_ex='MSB_2mgL_ex_weighted_average'
        MSB_em='MSB_2mgL_em_weighted_average'
        PPO_MSB='PPO_2gL+MSB_'+str(density)+'mgL_ex_275'

        Create_histogram(PC)
        Create_histogram(PPO)
        Create_histogram(MSB_ex)
        Create_histogram(MSB_em)
        Create_histogram(PPO_MSB)

        fitfunc=ROOT.TF1("fitfunc",Onetracklengthfunc, 300, 550, 4)
        fitfunc.SetParNames('PPO',"MSB_em",'MSB_ex',PC)

        c2 = ROOT.TCanvas("c2","MSB", 0, 0, 160*9, 90*9)
        c2.Divide(2,3)

        ROOT.gStyle.SetOptFit()

        Plot_histogram(PPO_MSB, 1)
        Plot_histogram(PC, 2)
        Plot_histogram(PPO, 3)
        Plot_histogram(MSB_ex, 4)
        Plot_histogram(MSB_em, 5)
        c2.cd(); c2.Modified(); c2.Update()
```